



Cite this: DOI: 10.1039/d6dt00831c

Synthesis of Lewis acid–base adducts between trimesityltriales and potassium cyanate and its heavier homologues

Kevin Dollberg, Mark Lochte, Pauline Weiß, Joel Nitzsche, Katalin Mészáros, Carsten von Hänisch  and Frank Tambornino *

Lewis acid–base adducts between trimesityltriales (MMes_3 ; Mes = 2,4,6-trimethylbenzene, M = Al–In) and potassium cyanate homologues (KNCE; E = O, S, Se) were synthesised in the presence of 18-crown-6 as an encapsulating agent. A series of compounds of the general composition $[\text{K}(18\text{c}6)(\text{thf})_{0-2}\text{ECN}(\text{MMes}_3)]$ was obtained and comprehensively characterised by multinuclear NMR spectroscopy, infrared spectroscopy, elemental analysis, and single-crystal X-ray diffraction. Structural analyses reveal systematic trends across both the triel and chalcogen series, while spectroscopic data provide insight into the electronic consequences of Lewis acid coordination. Complementary solubility studies demonstrate that adduct formation enhances the solubility of the otherwise poorly soluble potassium salts in selected solvents. The results highlight a class of Lewis acid–base adducts involving negatively charged cyanate and chalcogenocyanate fragments that has remained largely unexplored.

Received 10th April 2026,
Accepted 11th May 2026

DOI: 10.1039/d6dt00831c

rsc.li/dalton

Introduction

Salts of the cyanate anion (NCO^-) and its heavier chalcogen homologues, thiocyanate (NCS^-) and selenocyanate (NCSe^-), have been known for more than two centuries.¹ Since their earliest preparation, considerable attention has been devoted to the synthesis of additional metal salts and to exploiting their well-established pseudohalide character, as documented in several comprehensive reviews.^{2–7} Notably, the lighter representatives of this family have been investigated far more extensively than their heavier counterparts, both with respect to binary salt formation and subsequent reactivity patterns.^{1–12}

The chemistry of these ambident anions spans multiple areas of chemical science. In organic synthesis, cyanate and thiocyanate salts serve as versatile group-transfer reagents and play important roles in cyclisation processes leading to heterocyclic frameworks. In coordination chemistry, a broad range of transition-metal complexes incorporating NCO^- , NCS^- , and, to a lesser extent, NCSe^- ligands has been described, reflecting the diverse binding modes and electronic flexibility of these species.^{13–34}

In contrast to this rich coordination chemistry, the Lewis acid–base behaviour of these anions toward main-group electrophiles remains comparatively underexplored. Only isolated

examples demonstrate that cyanate and thiocyanate can function as Lewis bases in reactions with molecular Lewis acids, such as GaMe_3 or $\text{W}(\text{CO})_5$. For the selenocyanate anion, the available literature is even more limited and largely confined to transition-metal systems. This scarcity is notable given the fundamental role of Lewis acid–base interactions in controlling structure, bonding, and reactivity in main-group chemistry.

Recent studies have begun to highlight the broader relevance of such interactions. It was demonstrated that the related phosphathynolate anion (PCO^-) readily forms Lewis acid–base adducts with small triel electrophiles, illustrating how subtle variations in anionic electronic structure can influence bonding behaviour.^{35–38} These findings suggest that analogous chemistry might be accessible for the (heavy) cyanate anions, yet systematic investigations remain scarce (Fig. 1).

Motivated by this gap, and by the potential of Lewis acid coordination to modify the physicochemical properties of these salts, we set out to examine the interactions of potassium cyanate and its heavier homologues with representative triel Lewis acids. Particular emphasis was placed on identifying structural trends, spectroscopic signatures, and solubility effects associated with adduct formation.

Results and discussion

The required starting materials, namely the trimesityltriales (MMes_3 ; Al = **I**, Ga = **II**, In = **III**) and potassium selenocyanate

Fachbereich Chemie and Center for Quantum Materials and Sustainable Technologies, Philipps-Universität Marburg, Hans-Meerwein-Straße 4, 35043 Marburg, Germany. E-mail: tamborni@chemie.uni-marburg.de



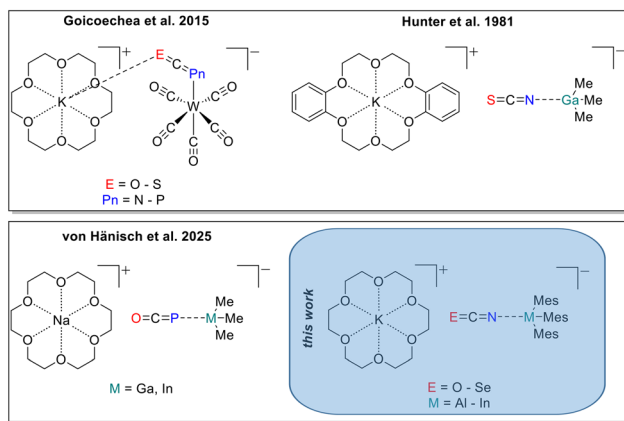
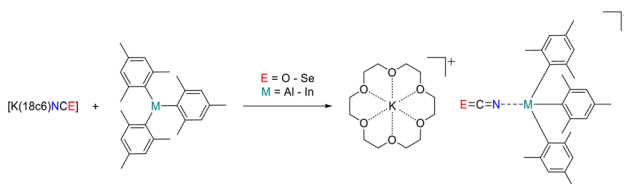


Fig. 1 Known Lewis acid–base adducts between related compounds of cyanates and Lewis acids.^{35,37,39}

(VI), were prepared according to literature procedures.^{38–42} The lighter homologues of potassium selenocyanate (KNCS; O = IV, S = V) were obtained commercially.

With the reactants in hand, the subsequent reactivity studies were undertaken. The reactivity of potassium thiocyanate was first examined following the scheme shown below. The desired Lewis acid–base adducts were generated by reacting the respective trimesityltriels with the potassium cyanates in the presence of 18-crown-6 (18c6) in 1,2-difluorobenzene (Scheme 1). Crystals of 1_{NCS} , 2_{NCS} , and 3_{NCS} suitable for single-crystal X-ray diffraction were obtained from THF/*n*-pentane mixtures at low temperature. All compounds crystallize in the triclinic space group $P\bar{1}$ with one formula unit in the asymmetric unit (Fig. 2). In each case, coordination of the nitrogen atom to the triel element is observed. The potassium cation is encapsulated by 18-crown-6 and further coordinated by THF.

Comparison of 1_{NCS} , 2_{NCS} , and 3_{NCS} reveals a clear periodic trend: the M–N distance increases markedly from 193.2(2) pm (1_{NCS}) to 235.1(4) pm (3_{NCS}), while the N–C bond length decreases from 116.5(2) pm to 100.3(6) pm over the same series. The C–S bond length increases by approximately 10 pm from 1_{NCS} to 3_{NCS} . The structural parameters of 1_{NCS} and 2_{NCS} closely resemble those reported for [K(crypt-222)NCS], where the anion is uncomplexed.⁴³ Additional comparisons can be drawn with related Al and Ga species reported in the literature, namely K[(AlMe₃)₂NCS] and [K(dibenzo-18c6)GaMe₃NCS].^{35,44} The Al analogue exhibits M–N and N–C distances very similar



Scheme 1 General synthesis of the compounds [K(18c6)(thf)_{0–2}ECN (MMe₃)] (M = Al–In; E = O–Se).

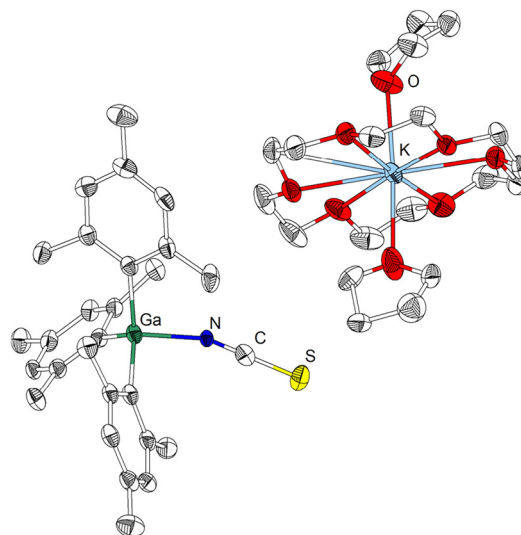


Fig. 2 Molecular structure of 2_{NCS} in the solid state. Hydrogen atoms are omitted for clarity. Ellipsoids are shown at a 50% probability level. Selected bond lengths (pm) and angles ($^{\circ}$) of 2_{NCS} : Ga–C 202.6(2), 202.3(2); Ga–N 203.7(2); N–C 114.7(3); C–S 163.5(2); C–Ga–N 99.04(7), 101.65(7), 103.51(7); Ga–N–C 160.0(2); N–C–S 178.9(2).

to those in 1_{NCS} , whereas detailed structural data for the Ga compound are not available.

For indium, fewer comparable structures exist, for example [(K(18c6))₃In(NCS)₆],⁴⁵ which differs substantially from 3_{NCS} , displaying a significantly shorter In–N distance (217(1) pm) and pronounced deviations in the N–C (114(2) pm) and C–S (160(1) pm) bond lengths.

The reactivity of potassium selenocyanate towards the triel starting materials was subsequently investigated. Following analogous procedures, the target adducts were obtained from reactions in 1,2-difluorobenzene, and crystals of 1_{NCSe} , 2_{NCSe} , and 3_{NCSe} suitable for X-ray diffraction were isolated from THF/*n*-pentane mixtures at low temperature. All compounds crystallize in the triclinic space group $P\bar{1}$ with one formula unit in the asymmetric unit (Fig. 3). As observed for the sulphur analogues, each structure features coordination of the nitrogen atom to the triel centre, and the potassium cation is encapsulated by 18-crown-6 and further coordinated by THF.

Across the series 1_{NCSe} to 3_{NCSe} , the M–N distance again increases significantly, from 193.8(2) pm to 228.6(3) pm, while the N–C bond length decreases from 116.0(3) pm to 111.9(4) pm. In contrast, the C–Se bond length shows only a slight elongation. Comparison with [Li(12c4)NCSe] indicates no substantial differences in the intrinsic structural parameters of the anion.⁴²

A survey of the literature reveals that studies on the Lewis basicity and coordination chemistry of the selenocyanate anion remain scarce. The available reports indicate that structural metrics of NCSe[–] are generally consistent across different systems.^{36,46,47}

Finally, attention was directed toward the reactivity of the lightest member of the series, the cyanate ion. Our investi-



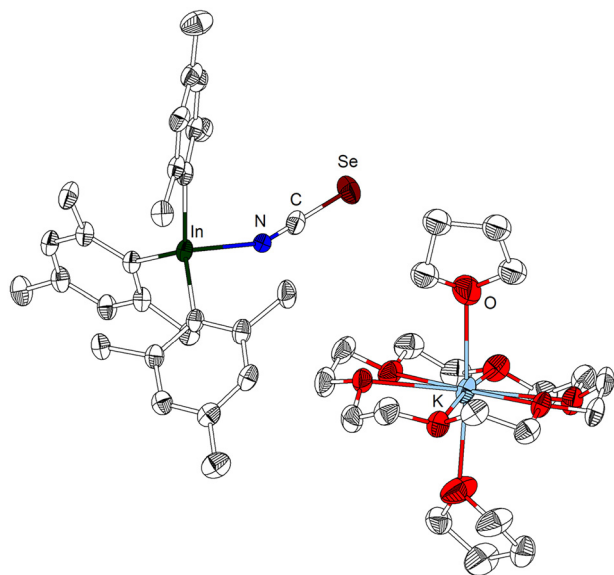


Fig. 3 Molecular structure of 3_{NCSe} in the solid state. Hydrogen atoms are omitted for clarity. Ellipsoids are shown at a 50% probability level. Selected bond lengths (pm) and angles ($^{\circ}$) of 3_{NCSe} : In–C 219.7(3), 220.4(3); In–N 228.6(3); N–C 111.9(4); C–Se 180.9(3); C–In–N 97.12(9), 100.63(9), 102.09(9); In–N–C 156.9(2); N–C–Se 178.7(3).

gations revealed that potassium cyanate exhibits markedly different behaviour compared to potassium thiocyanate and potassium selenocyanate. Compound 1_{NCO} was obtained from the reaction of **I** with **IV**, and crystals suitable for single-crystal X-ray diffraction were isolated from a mixture of 1,2-difluorobenzene and *n*-pentane. 1_{NCO} crystallizes in the orthorhombic space group *Pbca*. Owing to the absence of a donor solvent, this structure displays, for the first time in this study, a bridging interaction in which the anion links the Lewis acid to potassium, while the nitrogen atom remains coordinated to the triel centre (Fig. 4).

The quality of the crystallographic data permits only limited comparison with related structures reported in the literature. Nevertheless, the successful formation of pure 1_{NCO} is unambiguously supported by NMR spectroscopy, IR spectroscopy, and elemental analysis, *vide infra*.

Building on the synthesis of 1_{NCO} , attempts were made to prepare the heavier analogues 2_{NCO} and 3_{NCO} . In contrast to the systems described above, these reactions did not afford the desired products in high purity or yield. As part of our investigations, we carried out the aforementioned reactions in a wide variety of solvents, including 1,2-difluorobenzene, Et_2O , THF, toluene, and *n*-pentane. In addition, the reaction temperature was varied between $-78\text{ }^{\circ}\text{C}$ and room temperature. Various processing methods were also carried out in different temperature ranges. However, no reaction conditions were found under which a high yield or high purity of the target compounds could be obtained (see SI for details).

For 2_{NCO} , crystals suitable for X-ray diffraction were eventually obtained by slowly layering a one-to-one mixture of THF and 1,2-difluorobenzene with *n*-pentane over 3 months in an

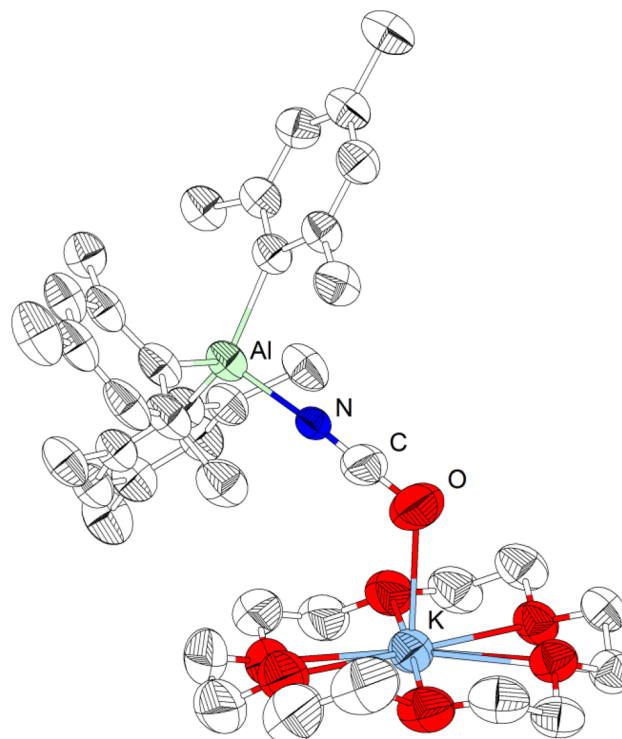


Fig. 4 Molecular structure of 1_{NCO} in the solid state. Hydrogen atoms are omitted for clarity. Ellipsoids are shown at a 50% probability level. Selected bond lengths (pm) and angles ($^{\circ}$) of 1_{NCO} : Al–C 203.2(4), 203.6(4), 204.4(3); Al–N 189.1(4); N–C 115.2(5); C–O 118.7(5); C–Al–N 99.2(2), 102.6(1), 110.4(2); Al–N–C 173.7(3); N–C–O 178.2(5).

H-shaped-Schlenk flask. Although the data quality is insufficient for detailed structural discussion, the presence of 2_{NCO} and the occurrence of a bridging motif analogous to that in 1_{NCO} can be confirmed. NMR spectroscopic data further support the formation of 2_{NCO} , although additional unidentified species are present due to incomplete purification.

A similar situation was encountered for 3_{NCO} . NMR spectroscopy indicates formation of the target compound, but purification proved unsuccessful. Crystallisation was challenging; however, a small number of crystals suitable for single-crystal X-ray analysis were ultimately obtained from THF/*n*-pentane. The structural data suggest mixed crystallisation of the desired product with $[\text{K}(18\text{c}6)(\text{thf})_2(\text{InMes}_3)\text{Cl}]$. These data apply only to the individual analysed crystal and do not allow conclusions regarding the composition of the bulk material. X-ray diffraction data suggests that the anion is coordinated to the Lewis acid *via* the oxygen atom. Isolation of 3_{NCO} in analytically pure form was not achieved (Table 1).

Spectroscopic studies

In addition to the crystallographic studies, the compounds were examined in more detail with respect to their spectroscopic signatures. As the cyanate homologues could not be obtained in satisfactory purity, the following discussion



Table 1 Comparison of selected atomic distances of compounds 1–3

Compound	M–N/pm	N–C/pm	C–E/pm
1 _{NCO}	189.1(4)	115.2(5)	118.7(5)
2 _{NCO}	—	—	—
3 _{NCO}	—	125.9	97.7
1 _{NCS}	193.2(2)	116.5(2)	161.7(2)
2 _{NCS}	203.7(2)	114.7(3)	163.5(2)
3 _{NCS}	235.1(4)	100.3(6)	171.7(7)
1 _{NCSe}	193.8(2)	116.0(3)	178.5(3)
2 _{NCSe}	204.6(1)	115.4(2)	178.5(2)
3 _{NCSe}	228.6(3)	111.9(4)	180.9(3)

focuses on the thiocyanate- and selenocyanate-containing species (1–3_{NCS}, 1–3_{NCSe}).

NMR spectroscopy was first employed to probe the influence of both the Lewis acid and the chalcogen on the chemical shift of the anionic ¹³C nucleus. A clear high-field shift is observed upon descending the chalcogen group (1_{NCS}: 137.39 ppm; 1_{NCSe}: 130.56 ppm). In contrast, variation of the triel centre exerts a much smaller effect, with compounds 1 and 3 displaying nearly identical ¹³C shifts (1_{NCS}: 137.39 ppm; 3_{NCS}: 137.69 ppm). This behaviour is consistent with the very similar electronegativities of aluminium (EN = 1.47) and indium (EN = 1.49). These trends agree well with literature reports.^{39,42,48–52} A comparison with the lighter cyanate analogues is not possible, as the ¹³C resonance of the anion could not be detected for any of the NCO compounds.

The ⁷⁷Se NMR data also provides some insight. A small difference of approximately 10 ppm is observed across 1_{NCSe}, 2_{NCSe}, and 3_{NCSe}. Relative to the starting material VI, all com-

pounds exhibit a low-field shift of at least 25 ppm.⁴² As the chemical shift range for ⁷⁷Se spans several thousand ppm these differences are, while following a clear trend, relatively small. This stems from the fact that the Se atom in the 1–3_{NCSe} is furthest from the triel, and thus least influenced by variation thereof.

IR spectra were recorded for all compounds (see SI for details). Comparison of the spectra shows that the C–N stretching vibration decreases markedly in frequency with increasing chalcogen period, in agreement with observations for related systems. Variations across the triel series, however, are considerably smaller; only a slight decrease in the stretching frequency is observed from Al to In. Overall, the measured vibrational frequencies fall within the range reported for comparable compounds (Table 2).^{39,53,54}

Solubility studies

The enhanced solubility of the Lewis acid–base adducts compared to the parent potassium salts represents one of the most notable practical consequences of adduct formation. To quantify this effect, the solubilities of potassium cyanate (IV), potassium thiocyanate (V), potassium selenocyanate (VI), and selected adducts (1_{NCO}, 1_{NCS}, 1_{NCSe}) were determined in a range of representative solvents (Table 3).

Potassium cyanate (IV) was found to be nearly insoluble in all investigated solvents, precluding reliable quantitative measurements. In contrast, adduct formation leads to measurable solubility, with 1_{NCO} exhibiting concentrations up to 0.096 mol L^{−1} in THF. This observation highlights the substantial impact of Lewis acid coordination and crown ether encapsulation on the physicochemical properties of the otherwise poorly soluble salt.

For potassium thiocyanate (V) and potassium selenocyanate (VI), clear solvent-dependent trends are observed. In donor solvents such as 1,2-dimethoxyethane and pyridine, both salts already display appreciable solubility. The corresponding Lewis acid–base adducts remain similarly or more soluble. For example, in pyridine, 1_{NCSe} reaches 0.488 mol L^{−1}, closely approaching the value measured for VI (0.545 mol L^{−1}), indicating that adduct formation does not compromise solubility even in strongly coordinating media.

More pronounced effects are evident in moderately coordinating solvents. In THF, where no reliable value for V could be obtained, 1_{NCS} and 1_{NCSe} display significant solubility (0.200 and 0.274 mol L^{−1}, respectively). Likewise, in 1,2-difluoroben-

Table 2 Comparison of selected NMR shifts and ν_1 stretching modes of compounds 1–3

Compound	¹³ C NMR shift ^a /ppm	⁷⁷ Se NMR shift ^a /ppm	ν_1 stretching ^b /cm ^{−1}
1 _{NCS}	137.39	—	2082
2 _{NCS}	135.72	—	2081
3 _{NCS}	137.69	—	2060
1 _{NCSe}	130.56	−341.4	2078
2 _{NCSe}	126.90	−330.9	2080
3 _{NCSe}	128.17	−331.1	2062

^a All NMR spectra are measured in THF-d₈ at room temperature with 300 MHz. ^b All IR spectra are measured under argon atmosphere at room temperature.

Table 3 Comparison of the solubility of IV–VI and 1_{NCO}–1_{NCSe} in different solvents. Potassium cyanate (IV) was almost insoluble in all solvents considered. The solvents *n*-pentane, diethyl ether, and dioxane showed no dissolution of the compounds considered

Compound	IV/mol L ^{−1}	IV-18c6/mol L ^{−1}	1 _{NCO} /mol L ^{−1}	V/mol L ^{−1}	V-18c6/mol L ^{−1}	1 _{NCS} /mol L ^{−1}	VI/mol L ^{−1}	VI-18c6/mol L ^{−1}	1 _{NCSe} /mol L ^{−1}
1,2-Dimethoxyethane	—	—	0.049	0.554	0.101	0.190	0.344	0.147	0.274
Tetrahydrofuran	—	—	0.096	—	0.032	0.200	0.120	0.023	0.274
Acetonitrile	—	0.065	0.043	0.203	0.218	0.058	0.445	0.222	0.156
Pyridine	—	—	0.090	0.115	0.080	0.243	0.545	0.093	0.488
1,2-Difluorobenzene	—	—	0.042	—	—	0.077	0.051	—	0.175



zene, the adducts exhibit clearly enhanced solubility relative to the parent salts, consistent with improved compatibility of the charge-diffuse, crown-ether-stabilised ion pairs with less polar environments.

Across the solvent series, the data reveal that solubility is primarily governed by solvent donor strength and polarity, yet the formation of Lewis acid–base adducts systematically broadens the accessible solvent window. This behaviour is readily rationalised by disruption of the extended ionic lattice typical of the simple potassium salts and by effective charge delocalisation within the crown-ether-encapsulated cation–anion assemblies.

Both the starting materials and the adducts show negligible solubility in non-polar or weakly coordinating solvents such as *n*-pentane and diethyl ether, indicating that lattice and ion-pairing effects remain dominant under these conditions.

Conclusions

This work describes the synthesis of hitherto unknown Lewis acid–base adducts formed between trimesityltriethers and potassium cyanates. The results demonstrate that previously unreported adducts can be obtained in good yields by reacting MMes_3 ($\text{M} = \text{Al–In}$) with $[\text{KNCE}]$ ($\text{E} = \text{O–Se}$) in the presence of 18-crown-6. The compounds were primarily characterised by multinuclear NMR spectroscopy and single-crystal X-ray diffraction, complemented by infrared spectroscopy and elemental analysis.

Furthermore, the solubility behaviour of selected representatives ($\mathbf{1}_{\text{NCO}}$, $\mathbf{1}_{\text{NCS}}$, and $\mathbf{1}_{\text{NCSe}}$) was systematically examined in various solvents. Adduct formation was shown to significantly enhance solubility compared to the parent potassium salts, highlighting the potential utility of these species as soluble cyanate transfer reagents.

Ongoing work is directed toward exploring the reactivity of the Lewis acid–base adducts and benchmarking their behaviour against that of the corresponding potassium cyanates. Emphasis is placed on reactions involving multiple-bond systems, where improved solubility and modified electronic properties are expected to influence reactivity.

Experimental section

All manipulations were carried out under argon atmosphere using standard Schlenk technique. All solvents used in the reactions and for crystallisations were dried *via* standard techniques, distilled and stored under argon. Solvents were never stored longer than three weeks before use. NMR spectra were recorded using a Bruker Avance II 300 MHz at 300 K. The IR spectra were run on a Bruker FT-IR spectrometer using the attenuated total reflectance (ATR) mode. Elemental analysis was performed on an Elementar Vario MicroCube. Single-crystal structure analyses were performed for compound $\mathbf{1}_{\text{NCO}}$ on a Stoe StadiVari X-ray diffraction system (Cu-K α ; Xenocs

Microfocus Source). For all other compounds crystal structure analysis were performed on a Bruker D8 Quest area detector system (Mo-K α ; Incoatec Microfocus Source). The data obtained were processed using X-Area for compound $\mathbf{1}_{\text{NCO}}$ and APEX3 for all other compounds. The crystal structures were refined using OLEX2-1.5.

$\mathbf{1}_{\text{NCO}}$: KNCO (100 mg, 1.23 mmol, 1.00 eq.) and 18c6 (324 mg, 1.23 mmol, 1.00 eq.) were suspended in 6 ml of 1,2-difluorobenzene. A solution of AlMe_3 (472 mg, 1.23 mmol, 1.00 eq.) in 6 ml of 1,2-difluorobenzene was then added at -30 °C. The reaction solution was subsequently warmed to room temperature and stirred for a further 2 hours. The clear, colourless solution was then mixed with 7 ml of *n*-pentane until a slight cloudiness developed. The reaction solution was then filtered and stored at -32 °C for crystallization. The crystals obtained in this way were separated from the supernatant solution by decanting and washed twice with *n*-pentane. $\mathbf{1}_{\text{NCO}}$ was obtained as a colourless solid (crystalline yield: 32%). $\text{C}_{40}\text{H}_{57}\text{AlKNO}_7$ calcd: C, 65.82; H, 7.87; N, 1.92; found: C, 65.97; H, 7.03; N, 1.71; ^1H NMR (300 MHz, THF- d_8) δ : 6.47 (s, 6H, *m-CH*), 3.53 (s, 24H, 18c6), 2.22 (s, 18H, *o-CH}_3*), 2.12 (s, 9H, *p-CH}_3*). $^{13}\text{C}\{^1\text{H}\}$ NMR (75 MHz, THF- d_8) δ : 154.36 (s, *i-C}_{\text{arom}}*), 146.88 (s, *o-C}_{\text{arom}}*), 133.67 (s, *p-C}_{\text{arom}}*), 127.09 (s, *m-C}_{\text{arom}}*), 71.16 (s, 18c6), 26.29 (s, *o-CH}_3*), 21.51 (s, *p-CH}_3*); IR (cm^{-1}): 3616 (w), 3006 (m), 2952 (m), 2910 (m), 2869 (m), 2723 (m), 2260 (s), 2203 (m), 1978 (m), 1710 (m), 1596 (m), 1535 (m), 1505 (m), 1451 (m), 1396 (m), 1372 (m), 1349 (m), 1284 (m), 1248 (m), 1219 (m), 1103 (s), 1027 (m), 961 (m), 841 (m), 806 (m), 754 (m), 618 (m), 585 (m), 561 (m), 550 (m), 498 (m), 454 (m).

$\mathbf{2}_{\text{NCO}}$: KNCO (100 mg, 1.23 mmol, 1.00 eq.) and 18c6 (324 mg, 1.23 mmol, 1.00 eq.) were suspended in 6 ml of 1,2-difluorobenzene. A solution of GaMe_3 (525 mg, 1.23 mmol, 1.00 eq.) in 6 ml of 1,2-difluorobenzene was then added at -30 °C. The reaction solution was subsequently warmed to room temperature and stirred for a further 2 hours. The clear, colourless solution was then mixed with 7 ml of *n*-pentane until a slight cloudiness developed. The reaction solution was then filtered and stored at -72 °C for crystallization. The crystals obtained in this way were separated from the supernatant solution by decanting and washed twice with *n*-pentane. $\mathbf{2}_{\text{NCO}}$ was obtained as a colourless solid. Crystals suitable for X-ray structural analysis on single crystals were obtained from a THF solution layered with *n*-pentane. ^1H NMR (300 MHz, THF- d_8) δ : 6.54 (s, 6H, *m-CH*), 3.58 (s, 24H, 18c6), 2.25 (s, 18H, *o-CH}_3*), 2.16 (s, 9H, *p-CH}_3*).

$\mathbf{3}_{\text{NCO}}$: KNCO (91 mg, 1.13 mmol, 1.00 eq.) and 18c6 (294 mg, 1.13 mmol, 1.00 eq.) were suspended in 6 ml of 1,2-difluorobenzene. A solution of InMe_3 (617 mg, 1.13 mmol, 1.00 eq.) in 6 ml of 1,2-difluorobenzene was then added at -30 °C. The reaction solution was subsequently warmed to room temperature and stirred for a further 2 hours. For purification, the solvent was removed under reduced pressure and the resulting colourless solid was dissolved in THF. Subsequently, *n*-pentane was added until the solution became cloudy. The suspension was then filtered and stored at -32 °C



for crystallization. 3_{NCO} could be isolated as a colourless solid (crystalline yield: 64%). $\text{C}_{40}\text{H}_{57}\text{InKNO}_7$ calcd: C, 58.75; H, 7.03; N, 1.71; found: C, 58.69; H, 6.88; N, 1.34; ^1H NMR (300 MHz, THF- d_8) δ : 6.61 (s, 6H, *m*-CH), 3.55 (s, 24H, 18c6), 2.33 (s, 18H, *o*-CH₃), 2.18 (s, 9H, *p*-CH₃). $^{13}\text{C}\{^1\text{H}\}$ NMR (75 MHz, THF- d_8) δ : 158.73 (s, *i*-C_{arom}), 146.44 (s, *o*-C_{arom}), 134.26 (s, *p*-C_{arom}), 126.63 (s, *m*-C_{arom}), 71.15 (s, 18c6), 26.78 (s, *o*-CH₃), 21.46 (s, *p*-CH₃); IR (cm⁻¹): 3006 (w), 2909 (m), 2861 (m), 2725 (m), 2204 (m), 1594 (m), 1543 (m), 1451 (m), 1398 (m), 1373 (m), 1350 (m), 1326 (m), 1284 (m), 1248 (m), 1222 (m), 1102 (s), 1027 (m), 960 (m), 912 (m), 840 (m), 707 (m), 617 (m), 577 (m), 539 (m), 491 (m).

1_{NCS} : KNCS (100 mg, 1.03 mmol, 1.00 eq.) and 18c6 (271 mg, 1.03 mmol, 1.00 eq.) were suspended in 6 ml of 1,2-difluorobenzene. A solution of AlMe₃ (396 mg, 1.03 mmol, 1.00 eq.) in 6 ml of 1,2-difluorobenzene was then added at -30 °C. The reaction solution was subsequently warmed to room temperature and stirred for a further 2 hours. The clear, colourless solution was then mixed with 7 ml of *n*-pentane until a slight cloudiness developed. The reaction solution was then filtered and stored at -32 °C for crystallization. The crystals obtained in this way were separated from the supernatant solution by decanting and washed twice with *n*-pentane. 1_{NCS} was obtained as a colourless solid (crystalline yield: 75%). Crystals suitable for X-ray structural analysis on single crystals were obtained from a THF solution layered with *n*-pentane at -72 °C. $\text{C}_{40}\text{H}_{57}\text{AlKNO}_6\text{S}$ calcd: C, 64.40; H, 7.70; N, 1.88; found: C, 64.31; H, 7.92; N, 1.79; ^1H NMR (300 MHz, THF- d_8) δ : 6.50 (s, 6H, *m*-CH), 3.55 (s, 24H, 18c6), 2.21 (s, 18H, *o*-CH₃), 2.13 (s, 9H, *p*-CH₃). $^{13}\text{C}\{^1\text{H}\}$ NMR (75 MHz, THF- d_8) δ : 152.40 (s, *i*-C_{arom}), 146.95 (s, *o*-C_{arom}), 137.39 (s, CNS), 134.23 (s, *p*-C_{arom}), 127.22 (s, *m*-C_{arom}), 71.20 (s, 18c6), 26.16 (s, *o*-CH₃), 21.51 (s, *p*-CH₃); IR (cm⁻¹): 3008 (w), 2943 (m), 2909 (m), 2082 (s), 1596 (m), 1538 (m), 1451 (m), 1402 (m), 1349 (m), 1282 (m), 1249 (m), 1219 (m), 1103 (s), 1058 (m), 1032 (m), 959 (m), 908 (m), 843 (m), 589 (s), 563 (m), 546 (m), 495 (m), 408 (m).

2_{NCS} : KNCS (100 mg, 1.03 mmol, 1.00 eq.) and 18c6 (271 mg, 1.03 mmol, 1.00 eq.) were suspended in 6 ml of 1,2-difluorobenzene. A solution of GaMe₃ (440 mg, 1.03 mmol, 1.00 eq.) in 6 ml of 1,2-difluorobenzene was then added at -30 °C. The reaction solution was subsequently warmed to room temperature and stirred for a further 2 hours. The clear, colourless solution was then mixed with 7 ml of *n*-pentane until a slight cloudiness developed. The reaction solution was then filtered and stored at -32 °C for crystallization. The crystals obtained in this way were separated from the supernatant solution by decanting and washed twice with *n*-pentane. 2_{NCS} was obtained as a colourless solid (crystalline yield: 71%). Crystals suitable for X-ray structural analysis on single crystals were obtained from a THF solution layered with *n*-pentane at -72 °C. $\text{C}_{40}\text{H}_{57}\text{GaKNO}_6\text{S}$ calcd: C, 60.91; H, 7.28; N, 1.78; found: C, 60.73; H, 7.34; N, 1.95; ^1H NMR (300 MHz, THF- d_8) δ : 6.60 (s, 6H, *m*-CH), 3.54 (s, 24H, 18c6), 2.29 (s, 18H, *o*-CH₃), 2.15 (s, 9H, *p*-CH₃). $^{13}\text{C}\{^1\text{H}\}$ NMR (75 MHz, THF- d_8) δ : 152.53 (s, *i*-C_{arom}), 145.85 (s, *o*-C_{arom}), 135.72 (s, CNS), 134.23 (s, *p*-C_{arom}), 127.44 (s, *m*-C_{arom}), 71.22 (s, 18c6), 25.76 (s, *o*-CH₃),

21.44 (s, *p*-CH₃); IR (cm⁻¹): 3009 (w), 2945 (m), 2909 (m), 2867 (m), 2081 (s), 1597 (m), 1545 (m), 1452 (m), 1404 (m), 1376 (m), 1350 (m), 1248 (m), 1102 (s), 1031 (m), 959 (m), 911 (m), 842 (m), 714 (m), 580 (m), 544 (m), 495 (m), 478 (m).

3_{NCS} : KNCS (100 mg, 1.03 mmol, 1.00 eq.) and 18c6 (271 mg, 1.03 mmol, 1.00 eq.) were suspended in 6 ml of 1,2-difluorobenzene. A solution of InMe₃ (486 mg, 1.03 mmol, 1.00 eq.) in 6 ml of 1,2-difluorobenzene was then added at -30 °C. The reaction solution was subsequently warmed to room temperature and stirred for a further 2 hours. The clear, colourless solution was then mixed with 7 ml of *n*-pentane until a slight cloudiness developed. The reaction solution was then filtered and stored at -32 °C for crystallization. The crystals obtained in this way were separated from the supernatant solution by decanting and washed twice with *n*-pentane. 3_{NCS} was obtained as a colourless solid (crystalline yield: 83%). Crystals suitable for X-ray structural analysis on single crystals were obtained from a THF solution layered with *n*-pentane at -72 °C. $\text{C}_{40}\text{H}_{57}\text{InKNO}_6\text{S}$ calcd: C, 57.62; H, 6.89; N, 1.68; found: C, 57.59; H, 6.97; N, 1.52; ^1H NMR (300 MHz, THF- d_8) δ : 6.60 (s, 6H, *m*-CH), 3.54 (s, 24H, 18c6), 2.29 (s, 18H, *o*-CH₃), 2.15 (s, 9H, *p*-CH₃). $^{13}\text{C}\{^1\text{H}\}$ NMR (75 MHz, THF- d_8) δ : 157.47 (s, *i*-C_{arom}), 146.36 (s, *o*-C_{arom}), 137.69 (s, CNS), 134.73 (s, *p*-C_{arom}), 126.80 (s, *m*-C_{arom}), 71.20 (s, 18c6), 26.73 (s, *o*-CH₃), 21.46 (s, *p*-CH₃); IR (cm⁻¹): 3008 (w), 2940 (m), 2907 (m), 2865 (m), 2823 (m), 2060 (s), 1594 (m), 1542 (m), 1452 (m), 1398 (m), 1373 (m), 1350 (m), 1282 (m), 1249 (m), 1222 (m), 1102 (s), 1058 (m), 1031 (m), 958 (m), 906 (m), 842 (m), 803 (m), 707 (m), 576 (m), 539 (m), 489 (m).

1_{NCSe} : KNCS_e (56 mg, 0.39 mmol, 1.00 eq.) and 18c6 (103 mg, 0.39 mmol, 1.00 eq.) were suspended in 6 ml of 1,2-difluorobenzene. A solution of AlMe₃ (150 mg, 0.39 mmol, 1.00 eq.) in 6 ml of 1,2-difluorobenzene was then added at -30 °C. The reaction solution was subsequently warmed to room temperature and stirred for a further 2 hours. The clear, colourless solution was then mixed with 7 ml of *n*-pentane until a slight cloudiness developed. The reaction solution was then filtered and stored at -32 °C for crystallization. The crystals obtained in this way were separated from the supernatant solution by decanting and washed twice with *n*-pentane. 1_{NCSe} was obtained as a colourless solid (crystalline yield: 65%). Crystals suitable for X-ray structural analysis on single crystals were obtained from a THF solution layered with *n*-pentane at -72 °C. $\text{C}_{40}\text{H}_{57}\text{AlKNO}_6\text{Se}$ calcd: C, 60.59; H, 7.25; N, 1.77; found: C, 61.02; H, 7.56; N, 1.64; ^1H NMR (300 MHz, THF- d_8) δ : 6.51 (s, 6H, *m*-CH), 3.56 (s, 24H, 18c6), 2.21 (s, 18H, *o*-CH₃), 2.13 (s, 9H, *p*-CH₃). $^{13}\text{C}\{^1\text{H}\}$ NMR (75 MHz, THF- d_8) δ : 151.82 (s, *i*-C_{arom}), 146.95 (s, *o*-C_{arom}), 134.43 (s, *p*-C_{arom}), 130.56 (s, CNS_e), 127.28 (s, *m*-C_{arom}), 71.21 (s, 18c6), 26.20 (s, *o*-CH₃), 21.51 (s, *p*-CH₃). ^{77}Se NMR (95 MHz, THF- d_8) δ : -341.36; IR (cm⁻¹): 3009 (w), 2910 (m), 2868 (m), 2078 (s), 1596 (m), 1538 (m), 1450 (m), 1402 (m), 1349 (m), 1283 (m), 1249 (m), 1219 (m), 1103 (s), 1058 (m), 1032 (m), 959 (m), 90 (m), 843 (m), 684 (m), 590 (m), 563 (m), 545 (m), 494 (m), 447 (m), 423 (m), 408 (m).

2_{NCSe} : KNCS_e (100 mg, 0.69 mmol, 1.00 eq.) and 18c6 (183 mg, 0.69 mmol, 1.00 eq.) were suspended in 6 ml of 1,2-



difluorobenzene. A solution of GaMe₃ (305 mg, 0.69 mmol, 1.00 eq.) in 6 ml of 1,2-difluorobenzene was then added at –30 °C. The reaction solution was subsequently warmed to room temperature and stirred for a further 2 hours. The clear, colourless solution was then mixed with 7 ml of *n*-pentane until a slight cloudiness developed. The reaction solution was then filtered and stored at –32 °C for crystallization. The crystals obtained in this way were separated from the supernatant solution by decanting and washed twice with *n*-pentane. **2_{NCSe}** was obtained as a colourless solid (crystalline yield: 47%). Crystals suitable for X-ray structural analysis on single crystals were obtained from a THF solution layered with *n*-pentane at –72 °C. C₄₀H₅₇GaKNO₆Se calcd: C, 57.49; H, 6.88; N, 1.68; found: C, 57.89; H, 7.21; N, 1.65; ¹H NMR (300 MHz, THF-*d*₈) δ: 6.55 (s, 6H, *m*-CH), 3.55 (s, 24H, 18c6), 2.20 (s, 18H, *o*-CH₃), 2.15 (s, 9H, *p*-CH₃). ¹³C{¹H} NMR (75 MHz, THF-*d*₈) δ: 151.96 (s, *i*-C_{arom}), 145.80 (s, *o*-C_{arom}), 134.47 (s, *p*-C_{arom}), 127.52 (s, *m*-C_{arom}), 126.90 (s, CNSe), 71.22 (s, 18c6), 25.79 (s, *o*-CH₃), 21.43 (s, *p*-CH₃). ⁷⁷Se NMR (95 MHz, THF-*d*₈) δ: –330.85; IR (cm^{–1}): 3009 (w), 2945 (m), 2908 (m), 2080 (s), 1597 (m), 1545 (m), 1451 (m), 1404 (m), 1377 (m), 1350 (m), 1283 (m), 1248 (m), 1102 (s), 959 (m), 911 (m), 842 (m), 714 (m), 580 (m), 544 (m), 495 (m), 432 (m), 414 (m).

3_{NCSe}: KNCSe (56 mg, 0.39 mmol, 1.00 eq.) and 18c6 (103 mg, 0.39 mmol, 1.00 eq.) were suspended in 6 ml of 1,2-difluorobenzene. A solution of InMe₃ (184 mg, 0.39 mmol, 1.00 eq.) in 6 ml of 1,2-difluorobenzene was then added at –30 °C. The reaction solution was subsequently warmed to room temperature and stirred for a further 2 hours. The clear, colourless solution was then mixed with 7 ml of *n*-pentane until a slight cloudiness developed. The reaction solution was then filtered and stored at –32 °C for crystallization. The crystals obtained in this way were separated from the supernatant solution by decanting and washed twice with *n*-pentane. **3_{NCSe}** was obtained as a colourless solid (crystalline yield: 89%). Crystals suitable for X-ray structural analysis on single crystals were obtained from a THF solution layered with *n*-pentane at –72 °C. C₄₀H₅₇InKNO₆Se calcd: C, 54.55; H, 6.52; N, 1.59; found: C, 54.33; H, 6.71; N, 1.55; ¹H NMR (300 MHz, THF-*d*₈) δ: 6.61 (s, 6H, *m*-CH), 3.55 (s, 24H, 18c6), 2.28 (s, 18H, *o*-CH₃), 2.15 (s, 9H, *p*-CH₃). ¹³C{¹H} NMR (75 MHz, THF-*d*₈) δ: 157.12 (s, *i*-C_{arom}), 146.32 (s, *o*-C_{arom}), 134.90 (s, *p*-C_{arom}), 128.17 (s, CNSe), 126.86 (s, *m*-C_{arom}), 71.21 (s, 18c6), 26.75 (s, *o*-CH₃), 21.45 (s, *p*-CH₃). ⁷⁷Se NMR (95 MHz, THF-*d*₈) δ: –331.14; IR (cm^{–1}): 3009 (w), 2945 (m), 2908 (m), 2080 (s), 1597 (m), 1545 (m), 1451 (m), 1404 (m), 1377 (m), 1350 (m), 1283 (m), 1248 (m), 1102 (s), 959 (m), 911 (m), 842 (m), 714 (m), 580 (m), 544 (m), 495 (m), 432 (m), 414 (m). IR (cm^{–1}): 3009 (w), 2939 (m), 2907 (m), 2865 (m), 2823 (m), 2063 (s), 1594 (m), 1543 (m), 1452 (m), 1398 (m), 1373 (m), 1349 (m), 1282 (m), 1249 (m), 1222 (m), 1102 (s), 1058 (m), 1029 (m), 958 (m), 907 (m), 842 (m), 707 (m), 657 (m), 619 (m), 576 (m), 539 (m), 489 (m), 427 (m).

Conflicts of interest

There are no conflicts to declare.

Data availability

The data supporting this article have been included as part of the supplementary information (SI). Supplementary information is available. See DOI: <https://doi.org/10.1039/d6dt00831c>.

CCDC 2545156–2545163 contain the supplementary crystallographic data for this paper.^{55a–h}

Acknowledgements

We are grateful to the DFG for financial support (HA 3466/11-1 and FT 1357/7-1). Special thanks go to Dockweiler Chemicals GmbH for donating numerous chemicals.

References

- 1 S. Hohloch and F. Tambornino, *Inorg. Chem.*, 2025, **64**, 12900–12917.
- 2 A. Norbury, *Adv. Inorg. Chem. Radiochem.*, 1975, **17**, 231–386.
- 3 M. Cliffe, *Inorg. Chem.*, 2024, **63**, 13137–13156.
- 4 T. Castanheiro, J. Suffert, M. Donnard and M. Gulea, *Chem. Soc. Rev.*, 2016, **43**, 494–505.
- 5 C. Wechwithayakhlung, D. Packwood, D. Harding and P. Pattanasattayavong, *J. Phys. Chem. Solids*, 2021, **154**, 110085.
- 6 A. Golub, H. Kohler and V. Skopenko, *Chemistry of Pseudohalides*, Elsevier, Amsterdam, 21st edn, 1986.
- 7 A. Golub and V. Skopenko, *Russ. Chem. Rev.*, 1965, **34**, 901–908.
- 8 J. L. Gay-Lussac, *Ann. Phys.*, 1816, **53**, 138–183.
- 9 F. Wöhler, *Ann. Phys.*, 1822, **71**, 95–103.
- 10 R. Porrett, *Memoir on the Prussic Acid*, London, 27th edn, 1809.
- 11 R. Porrett, *Philos. Trans. R. Soc. London*, 1814, **104**, 527–556.
- 12 J. J. Berzelius, *Traité de chimie minérale. végétale et animale*, 1845.
- 13 W. Chang, S. Liew and S. Tan, *Lett. Org. Chem.*, 2023, **20**, 877–882.
- 14 S. K. Elledge, H. L. Tran, A. H. Christian, V. Steri, B. Hann, F. D. Toste, C. Chang and J. Wells, *Proc. Natl. Acad. Sci. U. S. A.*, 2020, **117**, 5733–5740.
- 15 N. A. Mohamed, N. A. A. El-ghany, M. M. Fahmy and M. H. Ahmed, *Polym. Bull.*, 2014, **71**, 2833–2849.
- 16 R. Yefidoff-freedman, T. Chen, R. Sahoo, L. Chen, G. Wagner, J. Halperin, B. Aktas and M. Chorev, *ChemBioChem*, 2014, **15**, 595–611.
- 17 T. Kitamura, K. Nagata and T. Hiroshi, *Tetrahedron Lett.*, 1995, **36**, 1081–1084.
- 18 N. Iranpoor, H. Firouzabadi and R. Azadi, *Tetrahedron Lett.*, 2006, **47**, 5531–5534.



- 19 M. Lin, N. Karadkhelkar, Y. Li, L. M. Eubanks, W. H. Tepp, S. Pellett and K. D. Janda, *J. Med. Chem.*, 2025, **68**, 8796–8816.
- 20 E. C. Alyea, K. J. Fisher, R. P. Shakya and A. E. Vougioukas, *Synth. React. Inorg. Met.-Org. Chem.*, 1988, **18**, 163–178.
- 21 G. Hua, J. Du, D. B. Cordes, A. M. Z. Slawin and J. D. Woollins, *Tetrahedron*, 2015, **71**, 1792–1798.
- 22 M. Hojjatief, S. Muralidharan and H. Freiser, *Tetrahedron*, 1989, **45**, 1611–1622.
- 23 D. Combs and M. Rampulla, *J. Heterocycl. Chem.*, 1989, **26**, 1885–1886.
- 24 L. Konnert, B. Reneaud, R. Marcia de Figueiredo, J. Campange, F. Lamaty, J. Martinez and E. Colacino, *J. Org. Chem.*, 2014, **79**, 10132–10142.
- 25 K. Schierle-Arndt, D. Kolter, K. Danielmeier and E. Steckhan, *Eur. J. Org. Chem.*, 2001, **2001**, 2425–2433.
- 26 N. de Kimpe, M. Boelens and J. Declercq, *Tetrahedron*, 1993, **49**, 3411–3424.
- 27 J. Girmiene, D. Gueyrard, A. Tatibouet, A. Sackus and P. Rollin, *Tetrahedron Lett.*, 2001, **42**, 2977–2980.
- 28 N. Baig, R. Chandrakala, V. Sudhir and S. Chandrasekaran, *J. Org. Chem.*, 2010, **75**, 2910–2921.
- 29 D.-C. Li, J.-M. Dou, K.-Y. Ding, D.-Q. Wang, M.-J. Niu and Y. Liu, *Acta Chim. Sin.*, 2003, **61**, 110.
- 30 J. Pickardt and S. Dechert, *Z. Anorg. Allg. Chem.*, 1999, **625**, 153–159.
- 31 C. Camp, L. Chatelain, C. E. Kefalidis, J. Pecaut, L. Maron and M. Mazzanti, *Chem. Commun.*, 2015, **51**, 15454–15457.
- 32 S. P. Petrosyants and A. B. Ilyukhin, *Koord. Khim.*, 2007, **33**, 265–271.
- 33 N. Kitanovski, A. Golobic and B. Ceh, *Croat. Chem. Acta*, 2007, **80**, 127–134.
- 34 X.-M. Song, X.-Q. Huang, J.-M. Dou and D.-C. Li, *Acta Crystallogr., Sect. E: Struct. Rep. Online*, 2008, **64**, 489.
- 35 J. Atwood, R. D. Rodgers, D. C. Hrcir, M. J. Zaworotko and W. E. Hunter, *Acta Crystallogr., Sect. A*, 1981, **37**, C83.
- 36 D. Li, M. Du, J. Dou and D. Wang, *Z. Anorg. Allg. Chem.*, 2005, **631**, 178–181.
- 37 K. Dollberg, S. Seus, M. Knieling, F. Färber, R. Richter, J. Nitzsche, K. Meszaros, S. Ivlev, F. Weigend and C. von Hänisch, *Z. Anorg. Allg. Chem.*, 2025, **652**, e202500155.
- 38 A. Bodach, K. Bamford, L. Longobardi, M. Felderhoff and D. Stephan, *Dalton Trans.*, 2020, **49**, 11689–11696.
- 39 A. R. Jupp, M. B. Geeson, J. E. Mcgrady and J. M. Goicoechea, *Eur. J. Inorg. Chem.*, 2016, 639–648.
- 40 O. T. Beachley, M. R. Churchill, J. Pazik and J. Ziller, *Organometallics*, 1986, **5**, 1814–1817.
- 41 J. Leman and A. Barron, *Organometallics*, 1989, **8**, 2214–2219.
- 42 A. Shlyaykher, M. Ehmann, A. J. Karttunen and F. Tambornino, *Chem. – Eur. J.*, 2021, **27**, 13552–13557.
- 43 T. Alfheim, J. Dale, P. Groth and K. D. Krautwurst, *J. Chem. Soc., Chem. Commun.*, 1984, 1502–1504.
- 44 R. Shakir, M. J. Zaworotko and J. L. Atwood, *J. Organomet. Chem.*, 1979, **171**, 9–16.
- 45 A. B. Ilyukhin and S. P. Petrosyants, *Koord. Khim.*, 2009, **36**, 559–564.
- 46 T. Reinert, J. Boeckmann, I. Jess and C. Näther, *Acta Crystallogr., Sect. E: Struct. Rep. Online*, 2010, **66**, 70–71.
- 47 N. A. Semenov, D. E. Gorbunov, M. V. Shakhova, G. E. Salnikov, I. Y. Bagryanskaya, V. V. Korolev, J. Beckmann, N. P. Gritsan and A. V. Zibarev, *Chem. – Eur. J.*, 2018, **24**, 12983–12991.
- 48 K. Dollberg, N. Michel, H. Schmücker, S. Seus, C. Jakobi, R. Richter and C. von Hänisch, *Chem. – Eur. J.*, 2025, **31**, e202404199.
- 49 K. Dollberg, C. Jakobi, H. Schmücker, R. Richter, F. Weigend and C. von Hänisch, *Organometallics*, 2024, **43**, 2812–2820.
- 50 A. L. Allred and E. G. Rochow, *J. Inorg. Nucl. Chem.*, 1958, **5**, 264–268.
- 51 L. C. Allen, *J. Am. Chem. Soc.*, 1989, **111**, 9003–9014.
- 52 A. Mathias, *Tetrahedron*, 1965, **22**, 1073–1075.
- 53 A. Sabatini and I. Bertini, *Inorg. Chem.*, 1965, **4**, 959–961.
- 54 D. Swank and R. Willett, *Inorg. Chem.*, 1965, **4**, 499–501.
- 55 (a) CCDC 2545156: Experimental Crystal Structure Determination, 2026, DOI: [10.5517/ccdc.csd.cc2rffftg](https://doi.org/10.5517/ccdc.csd.cc2rffftg);
 (b) CCDC 2545157: Experimental Crystal Structure Determination, 2026, DOI: [10.5517/ccdc.csd.cc2rffvh](https://doi.org/10.5517/ccdc.csd.cc2rffvh);
 (c) CCDC 2545158: Experimental Crystal Structure Determination, 2026, DOI: [10.5517/ccdc.csd.cc2rffwj](https://doi.org/10.5517/ccdc.csd.cc2rffwj);
 (d) CCDC 2545159: Experimental Crystal Structure Determination, 2026, DOI: [10.5517/ccdc.csd.cc2rffxk](https://doi.org/10.5517/ccdc.csd.cc2rffxk);
 (e) CCDC 2545160: Experimental Crystal Structure Determination, 2026, DOI: [10.5517/ccdc.csd.cc2rffyl](https://doi.org/10.5517/ccdc.csd.cc2rffyl);
 (f) CCDC 2545161: Experimental Crystal Structure Determination, 2026, DOI: [10.5517/ccdc.csd.cc2rffzm](https://doi.org/10.5517/ccdc.csd.cc2rffzm);
 (g) CCDC 2545162: Experimental Crystal Structure Determination, 2026, DOI: [10.5517/ccdc.csd.cc2rfg0p](https://doi.org/10.5517/ccdc.csd.cc2rfg0p);
 (h) CCDC 2545163: Experimental Crystal Structure Determination, 2026, DOI: [10.5517/ccdc.csd.cc2rfg1q](https://doi.org/10.5517/ccdc.csd.cc2rfg1q).

